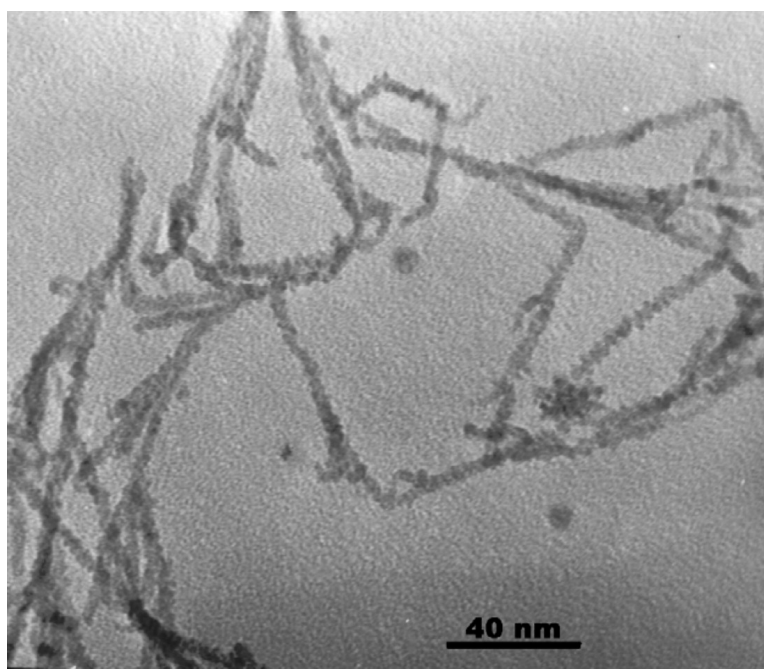Communication

Controlling Synthesis of BiIn Dendritic Nanocrystals by Solution Dispersion

Yanbao Zhao, Zhijun Zhang, Weimin Liu, Hongxin Dang, and Qunji Xue

More About This Article

Additional resources and features associated with this article are available within the HTML version:

- Supporting Information
- Access to high resolution figures
- Links to articles and content related to this article
- Copyright permission to reproduce figures and/or text from this article

View the Full Text HTML

Controlling Synthesis of BiIn Dendritic Nanocrystals by Solution Dispersion

Yanbao Zhao,[†,‡] Zhijun Zhang,*[,†] Weimin Liu,[‡] Hongxin Dang,[†] and Qunji Xue[‡]

Laboratory of Special Functional Materials, Henan University, Kaifeng Henan, 475002, China, and State Key Laboratory of Solid Lubrication, Lanzhou Institute of Chemical Physics, Chinese Academy of Sciences, Lanzhou 730000, China

Received December 16, 2003; E-mail: zhaoyb902@henu.edu.cn

Controlling synthesis of nanomaterials is an increasingly active area.[1,2] This interest arises from not only their unusual chemical and physical properties but also their potential application in many fields, which have stimulated the search for new synthetic methodologies for these materials. This is especially true for one-dimensional (1D) metallic materials, such as nanorods, nanowires, and nanotubes, which play a central role in the emerging area of nanotechnology.[3–5] In the past few years, great efforts have been devoted to the fabrication of 1D metallic nanomaterials, and several methods such as electron-beam induction,[6] electrochemical deposition,[7,8] thermal evaporation,[9,10] and surfactant-assisted reduction[11,12] have been developed. Among them, solution-phase methods appear to be of particular interest since they offer the potential of facile scale-up, and occur at moderate temperature. However, conventional solution methods often involve a series of complicated procedures and the use of expensive and sensitive agents. An alternative to obtain 1D metallic nanomaterials is to disperse melting metal in a suitable solvent, which may be simple and cheap.

We have been interested in using the solution-dispersion method for preparing zero-dimensional metallic nanoparticles.[13] The method is based on the microphase separation of a quasi-emulsion system, composed of melting metal and organic solvent. In this system, the shear stress τ tries to deform and break up the droplet, and it is counteracted by the surface tension σ.[14] A droplet of diameter d will break up when $\tau d/\sigma$ exceeds a critical value. Alternatively, the droplet will be elongated along shear stress, and the stress concentration and element segregation at the droplet surfaces should lead to the dendritic shapes. BiIn alloy has a low melting point and plays an important role in lubricants, protective materials, Pb-free solder, and thermal resist for microfabrication.[15] In this study, this methodology was extended to the synthesis of 1D nanocrystals. Here, we report the first preparation of soluble and dendritic BiIn nanocrystals from alloy ingot via the solution dispersion route.

In a typical experiment, 0.5 g of BiIn alloy ingot (melting point, 110 °C) was added to 40 mL of paraffin oil, the solution was sealed in 100-mL three-necked flasks equipped with magnetic stirring equipment, and the solution was heated to 220 °C and vigorously stirred for 7 h. Then, the suspension was cooled to room temperature, centrifuged, and washed with chloroform to obtain the dried product.

Figure 1 shows an X-ray diffraction (XRD) pattern of the BiIn dendritic nanocrystals prepared by solution dispersion. The XRD spectrum of BiIn dendritic nanocrystals contains multiple peaks that are clearly distinguishable. The peaks with 2θ values of 25.09°, 25.69°, 31.34°, 35.77°, 37.52°, 41.75°, 44.54°, 45.66°, 51.44°, 52.79°, and 56.11° correspond to the 110, 101, 111, 200, 002, 102, 211, 112, 220, 202, and 212 crystal planes of tetragonal phase BiIn ($a = 4.970$ Å, $c = 5.020$ Å, JCDPS, 85-0343), respectively. In the
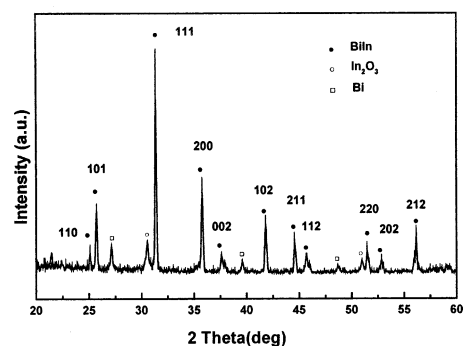

Figure 1. Powder X-ray diffraction (XRD) pattern of the as-obtained BiIn dendritic nanocrystals.
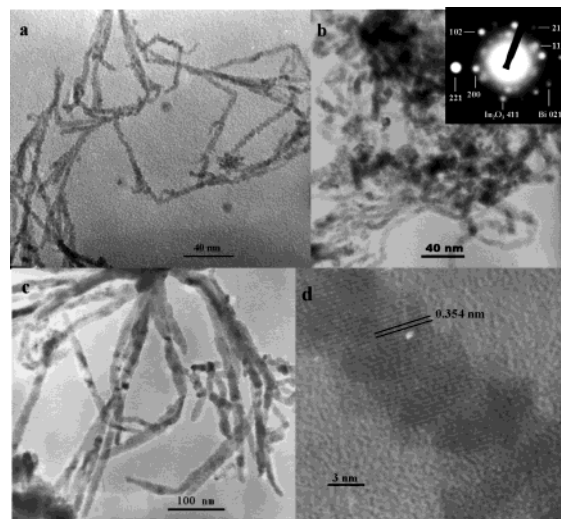

Figure 2. TEM images of various BiIn dendritic nanocrystals prepared at (a) 200 °C. (b) 200 °C. (c) 185 °C. (d) HRTEM image of an individual BiIn dendritic nanocrystal. The insert is the corresponding ED pattern.

XRD spectrum, there also appear weak additional peaks, which can be indexed to the crystalline Bi and In_2O_3, respectively. The XRD pattern proves that the resulting product is a mixture, which is predominantly composed of BiIn crystalline phase, with a small amount of crystalline Bi and In_2O_3.

Figure 2a shows a typical transmission electron microscopy (TEM) image of BiIn dendritic nanocrystals prepared by the solution-dispersion route at 220 °C, which is representative of the resulting products. It is clear that the resulting products have evident dendritic morphology, with an average diameter of 5 nm and an elongate shape, resulting in a large aspect ratio. The large aspect ratio might noticeably improve the solubility of the dendritic nanocrystals by absorbing solvent molecules. In addition, the size and morphology of BiIn alloy nanocrystals can be easily modified by adjusting the reaction parameters. The thicker dendritic nano-
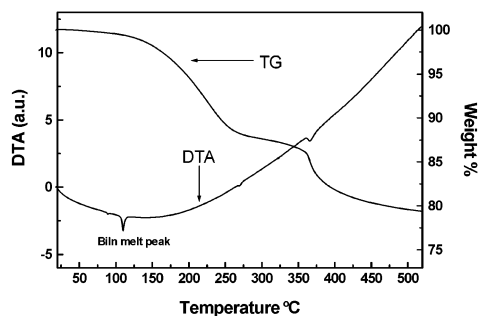
Figure 3. TG and DTA curves of BiIn nanocrystals prepared by the solution dispersion route.

Figure 4. Room-temperature photoluminescence (PL) spectra of dendritic samples and commercial In_2O_3 powders measured upon excitation at 260 nm.

crystals can be obtained at the relative lower reaction temperature. The nanocrystals of 10 nm in diameter were obtained at 200 °C (Figure 2b). The nanocrystals of 14 nm in diameter were also prepared at 185 °C (Figure 2c). The corresponding ED pattern (Figure 2b insert) exhibits discrete spots. Most of the spots can be easily indexed to the reflection for BiIn alloy, and some are assigned to the metal Bi and In_2O_3, which is consistent with the XRD results above. A high-resolution electron microscopy (HRTEM) image of a BiIn nanocrystal with a diameter of 7 nm is shown in Figure 2d. The visible lattice fringes in this image illustrate that the dendritic crystal is an approximately single crystal. The interplanar spacing is about 0.354 nm, which corresponds to the {110} plane of the tetragonal BiIn, revealing that the dendritic crystals consist of BiIn alloy. To study the In_2O_3 and Bi in the mixture, the dendritic crystals were dispersed in paraffin oil and stirred at 230 °C for 4 h in air atmosphere. It is clear that the oxidizing samples appear with a particle-like shape (Supporting Information, SI), indicating the formation of In_2O_3 particles although it is very difficult to distinguish Bi particles from In_2O_3 by our TEM study.

Figure 3 gives DTA/TG curves of the BiIn nanocrystals. As the temperature increases, the DTA curve presents one endothermic region and several endothermic peaks. The endothermic region in the range of room temperature to 250 °C, accompanying a marked mass loss, can be attributed to the release of small organic molecules from the sample powder. The endothermic peak at 110 °C corresponds to the melting of BiIn alloy, and the weaker decalescence at 270 °C indicates the presence of a little mount of Bi. The peak at 360 °C, accompanying a distinct weight loss, might be assigned to the further release of solvent molecules. In the TG curve, the sample presents two successive weight-loss processes from room temperature to 500 °C. The total weight loss is about 21%, indicating that at least 21% of organic molecules are absorbed on the nanocrystal surfaces, which can prevent further oxidation of BiIn dendritic nanocrystals.

The photoluminescence (PL) emission spectrum of the bulk dendritic samples was measured at room temperature using a Xe lamp upon excitation at 260 nm (4.76 eV). For comparison, the PL feature of commercial In_2O_3 powders was also given. As shown in Figure 4, an ultraviolet emission with peak at 412 nm was observed for commercial In_2O_3 powders. A striking PL feature showing in the dendritic samples is that there exists a strong ultraviolet emission band centered at 375 nm and a marked shoulder at 392 nm. Compared to the PL of In_2O_3 powders, the PL of the dendritic samples shows a blue shift of about 37 nm. Moreover,
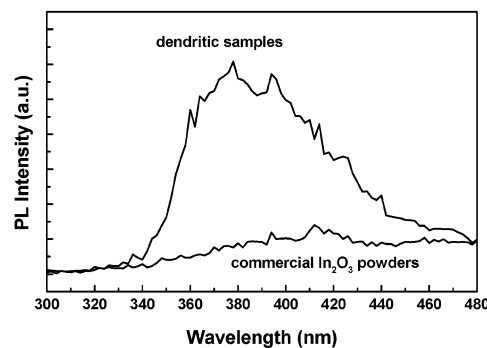
UV emission from dendritic samples was more than 6 times higher than that for commercial In_2O_3 powders. It is known that the metallic indium and bismuth cannot emit light at room temperature. This strong UV emission might arise from the In_2O_3 fine particles in the mixture, and the possible PL mechanism was related to quantum confinement effect (the critical Bohr radius of In_2O_3 is about 2.14 nm) because the size of In_2O_3 particles might be in the quantum confinement regime.

In conclusion, we report a novel solution method for controlling synthesis of metal dendritic nanocrystals and that the as-obtained BiIn nanocrystals have high crystalline and good solubility. The product through this technique is cheaper, and the morphology of the nanocrystals can be greatly modified by changing the reaction parameters. This strong UV emission might arise from the quantum-confined In_2O_3 particles.

Supporting Information Available: The TEM image and EDX spectrum of the oxidizing sample. This material is available free of charge via the Internet at http://pubs.asc.org.

References

(1) Keating, C. D.; Natan, M. J. *Adv. Mater.* **2003**, *15*, 451−454.
(2) Patzke, G. R.; Krumeich, F.; Nesper, R. *Angew. Chem., Int. Ed.* **2002**, *41*, 2447−2461.
(3) Sun, Y.; Mayers, B.; Xia, Y. *Adv. Mater.* **2003**, *15*, 641−646.
(4) Hermanson, K. D.; Lumsdon, S. O.; Williams, J. P.; Kaler, E. W.; Velev, O. D. *Science* **2001**, *294*, 1082−1086.
(5) Penner, R. M. *J. Phys. Chem. B* **2002**, *106*, 3339−3353.
(6) Edmondson, M. J.; Zhou, W.; Sieber, S. A.; Jones, I. P.; Gameson, I.; Anderson, P. A.; Edwards, P. P. *Adv. Mater.* **2001**, *13*, 1608−1611.
(7) Walter, E. C.; Zach, M. P.; Favier, F.; Murray, B. J.; Inazu, K.; Hemminger, J. C.; Penner, R. M. *ChemPhysChem* **2003**, *4*, 131−138
(8) Wang, Y. W.; Zhang, L. D.; Meng, G. W.; Peng, X. S.; Jin, Y. X.; Zhang, J. *J. Phys. Chem. B* **2002**, *106*, 2502−2507.
(9) Liu, Z.; Bando, Y. *Adv. Mater.* **2003**, *15*, 303−305.
(10) Li, Y.; Bando, Y.; Golberg, D. *Adv. Mater.* **2003**, *15*, 581−585.
(11) Xiong, Y.; Xie, Y.; Wu, C.; Yang, J.; Li, Z.; Xu, F. *Adv. Mater.* **2003**, *15*, 405−408.
(12) Soulantica, K.; Maisonnat, A.; Senocq, F.; Fromen, M. C.; Casanove, M. J.; Chaudret, B. *Angew. Chem., Int. Ed.* **2001**, *40*, 2984−2986.
(13) Zhao, Y. B.; Zhang, Z. J.; Dang, H. X. *J. Phys. Chem. B* **2003**, *107*, 7574−7576.
(14) Mohan, S.; Agarwala, V.; Ray, S. *Mater. Sci. Eng. A* **1991**, *144*, 215−219.
(15) Sarunic, M. V.; Chapman, G. H.; Tu, Y. *Proc. SPIE* **2001**, *4272*, 183−193.

JA031735H